Dilepton production by neutrinos in the Fermilab 15-foot bubble chamber

H. C. Ballagh, H. H. Bingham, T. Lawry, G. R. Lynch, J. Lys, J. Orthel,* M. D. Sokoloff, M. L. Stevenson, and
G. P. Yost

Department of Physics and Lawrence Berkeley Laboratory, University of California, Berkeley, Berkeley, California 94720

D. Gee, G. Harigel,† F. R. Huson, E. Schmidt, W. Smart, and E. Treadwell

Fermi National Accelerator Laboratory, P.O. Box 500, Batavia, Illinois 60510

R. J. Cence, F. A. Harris, M. D. Jones, S. I. Parker, M. W. Peters, V. Z. Peterson, and V. J. Stenger

Department of Physics, University of Hawaii at Manoa, Honolulu, Hawaii 96822

T. H. Burnett, L. Fluri,‡ H. J. Lubatti, K. Moriyasu, D. Rees, G. M. Swider,§ B. S. Yuldashev,¶ and E. Wolin

Visual Techniques Laboratory, Department of Physics, University of Washington, Seattle, Washington 98195

U. Camerini, W. Fry, R. J. Loveless, P. McCabe, M. Ngai, and D. D. Reeder

Department of Physics, University of Wisconsin, Madison, Wisconsin 53706

(Received 11 February 1981)

In an exposure of the Fermilab 15-foot neon-hydrogen bubble chamber to a quadrupole triplet neutrino beam, 49 $\mu^- e^+$ and 14 $\mu^+ e^-$ events with $e^\pm$ momenta greater than 0.3 GeV/c have been observed, yielding μe rates per charged-current event of $(0.73 \pm 0.11)\%$ and $(1.1 \pm 0.3)\%$, respectively. The $\mu^- e^+$ rate shows no strong energy dependence in the range from 30 to 300 GeV. The 18 neutral strange particles observed in the 63 events contain 14 K_S^0, 2 Λ, and 2 Λ/K_S^0 ambiguities, suggesting that the events are predominantly D-meson production and decay and that the $\Lambda_c^+ \to \Lambda e X$ branching ratio is very small. The corrected numbers of neutral strange particles per $\mu^- e^+$ and $\mu^+ e^-$ event are 1.2 ± 0.3 and $0.6^{+0.6}_{-0.3}$, respectively. Properties of the events, including strange-particle production, are compared to $\mu^\mp \mu^\pm$ events in the same experiment and to a charm production and decay model, and good agreement is found, apart from a possible enhancement at ~ 5–6 GeV/c^2 in the mass of the system recoiling against the μ^+ in $\mu^+ e^-$ (and $\mu^+ \mu^-$) events. As reported previously, four events show short-lived-particle decays, and D-meson lifetime estimates are reevaluated using the final event sample. One $\mu^+ e^+$ and three $\mu^- e^-$ events were observed. The $\mu^- e^-$ events are consistent with background and lead to a $\mu^- e^-/\mu^- e^+$ ratio of less than 0.07 (90% confidence level) for $e^\pm$ momenta above 0.8 GeV/c. Five candidates for dilepton production by electron neutrinos and antineutrinos in the beam are consistent with approximately 1% rates. No good three-lepton candidates were found, and one, previously reported, four-lepton candidate was found.

I. INTRODUCTION

Opposite-sign μe events have been observed previously in several bubble-chamber experiments.[1-9] These events and opposite-sign dimuon events observed by this[10] and some other bubble-chamber experiments[6, 11, 12] and by several counter experiments[13-17] have been interpreted as evidence for the production and subsequent semileptonic decay of charmed particles. Additional evidence from bubble chambers for the charm hypothesis comes from the observation of neutral-strange-particle decays associated with these events at a rate significantly higher than the rate in charged-current interactions.

No evidence for electron-neutrino–induced dilepton events has been reported previously, and only one experiment has reported evidence for $\mu^- e^-$ events.[18] Both are expected from μ-e universality; $\mu^- e^-$ events insofar as $\mu^- \mu^-$ events have been detected in counter experiments.[19, 20]

This experiment differs from many of the previous bubble-chamber experiments in that the incident neutrino energy is relatively high (the average ν event energy is 90 GeV) and the two-plane external muon identifier (EMI) makes muon identification very clean. The latter allows the study of μe and $\mu \mu$ dilepton events in the same experiment with high detection efficiencies for both muons and electrons. Apart from finite-mass effects, the two processes should be the same. Experimentally the processes have different backgrounds and detection efficiencies, and it is advantageous to study both.

An important limitation in experiments studying dimuon events, both with bubble chambers and with counters, is that for muon momenta below ~ 4 GeV/c the detection efficiency becomes small and background becomes large, so that results are given only for muon momenta above ~ 4 GeV/c. In contrast, primary electrons can be detected in the bubble chamber with high efficiency and low background down to ~ 0.3 GeV/c. In the present experiment the proportion of μe events in which the electron momentum is below 4 GeV/c is about 40%.

Experimental details and results on dimuon

events from this experiment have been reported previously.[10] In the present paper, we give brief descriptions of the apparatus (Sec. II) and muon identification (Sec. III) and then more detailed descriptions of electron identification (Sec. IV), electron background and losses (Sec. V), and detection efficiency and energy corrections (Sec. VI). In Sec. VII we present rates for $\mu^- e^+$ and $\mu^+ e^-$ events, plus associated V^0 rates. Also in Sec. VII, we discuss evidence for $e^+ e^-$, $e^- e^+$, and $e^- \mu^+$ events and for the like-sign channels, $\mu^- e^-$ and $\mu^+ e^+$. (Here and in general throughout the paper the first-named lepton is the "leading" lepton.) Finally in Sec. VII, we report on three- and four-lepton searches. In Sec. VIII, we compare properties of the $\mu^- e^+$ and $\mu^+ e^-$ events to a charm production and decay model; in looking at associated strange-particle properties, we include $\mu^- \mu^+$ and $\mu^+ \mu^-$ events. In Sec. IX, we reexamine our earlier D^0 and D^+ lifetime estimates that make use of observed short-lived-particle decays. Summary and conclusions are given in Sec. X.

II. APPARATUS

The experiment was carried out using the Fermilab 15-foot bubble chamber plus a two-plane external muon identifier.[21,22] The bubble-chamber liquid was a neon (47% atomic) -hydrogen mixture with a density, radiation length, and absorption length of 0.56 g/cm^3, 53 cm, and 193 cm, respectively. The bubble chamber was exposed to the quadrupole triplet neutrino beam. In this beam, the ratio of neutrino- to antineutrino-induced events is about 6 to 1, and the average event energies are 90 GeV for neutrinos and 60 GeV for antineutrinos. The electron-neutrino and -antineutrino components of the beam are measured to be 2% and 0.6%, respectively. A total of 326 000 pictures was obtained, corresponding to 3.4×10^{18} 400-GeV protons on target. The fiducial volume used in the present study was 14.5 m^3, giving a mass of 8.1 metric tons.

III. MUON IDENTIFICATION

Muons from events in the bubble chamber were identified using a combination of bubble-chamber and EMI information.[21,22] To be classified as a muon, a track was required to leave the bubble chamber without interacting and to have time-coincident matches in both EMI planes with a combined two-plane confidence level greater than 1%. This confidence level describes the goodness of fit of the EMI matches. A typical muon traverses 7 to 11 collision lengths of absorber. Only muons with momenta greater than 4 GeV/c were considered; at lower momenta the hadron con-

tamination of muons becomes large and the EMI geometrical acceptance becomes small. With the 4-GeV/c cut, the hadron contaminations of μ^- and μ^+ are 0.2% and 1.5%, respectively, while the product of EMI chamber efficiency and geometric acceptance is 0.72 for μ^- and 0.78 for μ^+.

With the above muon criteria, totals of 8900 neutrino and 1493 antineutrino charged-current events were identified within the fiducial volume.

For the dimuon sample, a somewhat larger fiducial volume of 17.6 m^3 was used (the minimum distance of events from the downstream wall of the bubble chamber was 50 cm rather than 70 cm). Totals of 54 opposite-sign dimuon candidates, 8 $\mu^- \mu^-$ candidates, and 0 $\mu^+ \mu^+$ candidates were found, with estimated backgrounds of 18, 7, and 1 events, respectively.[10]

For the μe sample, the contamination due to ν_e and $\bar{\nu}_e$ events with fake muons is quite small. For a hadron that does not interact in the bubble chamber and that extrapolates to intersect both EMI planes, the probability of being classified as a muon is 0.5%. The main contribution to this probability comes from unseen decays; punch through and accidentals provide a much smaller contribution. In the fiducial volume there are approximately 270 ν_e and 70 $\bar{\nu}_e$ events with identified electrons. The resulting estimates of $e\mu$ candidate events with a fake muon are 0.6, 0.3, 0.1, and 0.1 for $e^- \mu^+$, $e^- \mu^-$, $e^+ \mu^-$, and $e^+ \mu^+$, respectively.

IV. ELECTRON IDENTIFICATION

The 15-foot bubble chamber filled with a 47%-atomic-neon–hydrogen mixture is an excellent electron detector. Tracks from events in the fiducial volume have a potential length of at least 1.3 radiation lengths; most tracks are several radiation lengths long. Thus, electrons with an energy of less than a few GeV often both visibly radiate photons, which convert to $e^+ e^-$ pairs, and spiral to an end in the chamber. High-energy electrons create large showers of converted photons.

All tracks from the primary vertex of each neutral induced event were followed to their endpoints. Interacting tracks were assumed to be hadrons. Other tracks were examined for the following signatures: (1) visible change in curvature without change in direction, (2) electron pair, triplet, or Compton electron tangent to the track, (3) trident with energy greater than 10% of the energy of the track, (4) δ ray with energy greater than 25% of the energy of the track, (5) annihilation of positive track with tangent electron pair(s), and (6) spiraling to an end in the chamber.

In order to reduce backgrounds, tracks classi-

fied as primary electrons were required to have two or more signatures and a momentum greater than 300 MeV/c. The requirements to classify a track as part of a Dalitz decay (or close e^+e^- pair) were less stringent. Two tracks of opposite charge with one or more electron signatures each and with an invariant mass of less than 300 MeV/c^2 were classified as a Dalitz pair. Also, if a primary electron formed an invariant mass of less than 150 MeV/c^2 with an oppositely charged leaving track (of less than 150 cm in length), the two tracks were classified as a Dalitz pair.

The probability that an electron has at least two signatures was determined from a Monte Carlo simulation and also from a study of electrons in electron pairs associated with events. The average probability rises rapidly with electron energy: 0.40 at 300 MeV, 0.75 at 800 MeV, and 0.95 for energy greater than 5 GeV. A double scan of 50% of the events for electron candidates gives an overall electron scan efficiency of 0.95 ±0.05. Rates calculated for events with primary electrons are corrected for both the electron detection probability and the electron scan efficiency.

In about 2% of the charged-current events, it is not possible to determine if a direct electron is present, generally because of large multiplicity or poor visibility. We have used the observed distributions for μe and charged-current events to estimate that μe events are only about 1.2 times more likely to be in this sample than are charged-current events. Since the events lost are only slightly biased in favor of μe events and since the overall fraction is small, the correction to the μe rates is small.

Using the above selection criteria for events with primary electrons (which are not part of a Dalitz pair), we have identified 49 events with both a μ^- and an e^+, 16 events with both a μ^+ and an e^-, and 1 event with a μ^+ and an e^+. With the additional requirement that the momentum of the electron be greater than 0.8 GeV/c, we have 3

events with a μ^- and an e^-. Three events were found with an e^+ and an e^- (momentum greater than 0.3 GeV/c) and an invariant mass of greater than 0.8 GeV/c^2 and no muon of either charge.

V. ELECTRON BACKGROUNDS AND LOSSES

The main sources of background in the primary $e^\pm$ are asymmetric Dalitz pairs, asymmetric close γ conversions, Compton electrons, δ rays, and $K_{e3}^\pm$ decays. The estimated numbers of background $e^\pm$ from each source are given in Table I, for each μe charge state and for two $e^\pm$ momentum intervals. Other sources considered and summed into "other" in the table are β decays of hyperons and neutral kaons and zero charged-prong $\pi^\pm$-neon interactions with an appropriate Dalitz pair or close γ conversion.

The background estimates assumed average rates, per μ^- and μ^+ event, respectively, of 4.3 and 3.1 primary γ's, 0.17 and 0.15 primary K^+, and 0.11 and 0.06 primary K^-. The rates and spectra of γ's followed from assuming that the π^0 rates and spectra were equal to the averages of those for π^+ and π^-; similar results were obtained from the numbers of (nonbremsstrahlung) e^+e^- pairs observed at 10−30 cm pointing toward the primary vertex, and similar spectra were also obtained from the observed Dalitz pairs plus close γ conversions. The $K^\pm$ rates were obtained from the observed K_S^0 and Λ rates, after assuming equal rates for ΛK^0, ΛK^+, $\Sigma^\pm K^0$, and $\Sigma^\pm K^+$ production and for the four $K\bar{K}$ charge states and after allowing for strange particles resulting from charm decays. The $K^\pm$ spectra were assumed to be equal to the K_S^0 spectra. The background estimates also assumed that the following cases were misidentified as primary $e^\pm$: (a) asymmetric e^+e^- pairs occurring less than 1 cm from the primary vertex and with one partner having a momentum less than 5 MeV/c; (b) Compton electrons or δ rays on primary hadrons occurring less than 2

TABLE I. Background $e^\pm$ in μe events (numbers of events[a]).

μe charges P_e (GeV/c)	$\mu^- e^-$		$\mu^- e^+$		$\mu^+ e^-$		$\mu^+ e^+$	
	0.3−0.8	>0.8	0.3−0.8	>0.8	0.3−0.8	>0.8	0.3−0.8	>0.8
Asymmetric Dalitz pairs	0.3	0.1	0.3	0.1	0.1	0.0	0.1	0.0
Asymmetric $\gamma \to e^+e^-$ pairs	0.8	0.3	0.8	0.3	0.1	0.0	0.1	0.1
Compton electrons	6.9	3.1			0.9	0.4		
δ rays	2.1	0.6			0.2	0.1		
$K^\pm \to e^\pm \pi^0 \nu$ decays	0.1	0.5	0.1	0.8	0.0	0.0	0.0	0.1
Other[b]	0.1	0.1	0.1	0.2	0.0	0.0	0.0	0.0
Total	10.3	4.7	1.3	1.4	1.3	0.5	0.2	0.2

[a]Not corrected for $e^\pm$ scanning and two-signature inefficiencies.
[b]See text.

cm from the primary vertex; and (c) $K^{\pm} \to e^{\pm} \pi^0 \nu$ decays with a projected angle between $K^{\pm}$ and $e^{\pm}$ of less than 4°. Uncertainties in these average distances and angles and in the $K^{\pm}$ rates lead to an estimated 30% uncertainty in the final background numbers.

The numbers in Table I show that for e^- the most important background source is Compton electrons, while for e^+ the most important source is asymmetric e^+e^- pairs at low e^+ momentum and $K^+ \to e^+$ decays at high momentum.

Two causes of loss of good primary $e^{\pm}$ are: (i) a close δ ray on a primary track can make a primary e^+ look like a partner in a Dalitz pair or a close e^+e^- pair; (ii) a leaving primary hadron with length less than 150 cm and a small opening angle with a primary $e^{\pm}$ can appear to be a Dalitz pair partner (if the relevant effective mass is less than 150 MeV). Estimates of the resulting fractional losses of μe events are given in Table II. For the δ-ray case it was assumed that on average a δ ray within 1.2 cm of the primary vertex and with a momentum greater than 5 MeV/c would be misidentified; the 1.2 cm was determined after studying events on the scanning table. For the leaving hadron case it was assumed that the distribution in angle between a primary $e^{\pm}$ and a leaving hadron was the same as that between a primary $\pi^{\pm}$ and a leaving hadron. In both cases the assumptions are appropriate if the $e^{\pm}$ is the nonleading lepton. For the leaving hadron case, the loss rates depend on the numbers of leaving hadrons of the appropriate charge; the ratio of positive to negative leaving hadrons is approximately 2 to 1 in ν-induced events and approximately 1 to 1 in $\bar{\nu}$-induced events. These losses had no significant momentum dependence. The estimated uncertainty in the loss rates is 30% of the loss.

VI. DETECTION EFFICIENCIES AND ELECTRON- AND HADRON-ENERGY CORRECTIONS

Before determining rates, the detection efficiencies for charged-current and dilepton events must be determined. Because of correlations, the μe efficiency is not a simple product of μ and e

TABLE II. Fractional losses of μe events.

μe charges	$\mu^- e^-$	$\mu^- e^+$	$\mu^+ e^-$	$\mu^+ e^+$
$e^+ + \delta$ ray $\to e^+e^-$ pair		0.06		0.06
$e^{\pm}$ + leaving hadron $\to e^+e^-$ pair	0.05	0.02	0.02	0.02

efficiencies. We have used a Monte Carlo program to move dilepton events and charged-current events randomly about the bubble chamber and rotate them randomly about the neutrino direction. The muon acceptance for each charged current event is then determined from the fraction of Monte Carlo generated events where the extrapolated muon strikes the EMI. To determine the acceptance for a μe event, the sum of the electron detection efficiencies for those Monte Carlo-generated events where the extrapolated muon strikes the EMI is divided by the total number of generated events. The electron detection efficiency, which is the probability of obtaining two electron signatures (see Sec. IV), is obtained from a Monte Carlo generated lookup table, which is parametrized in terms of electron energy and path length to the bubble-chamber wall. This table has been checked against an experimental determination of the electron detection efficiency using electrons and positrons from γ conversions in the bubble chamber. The final efficiencies, including muon acceptance, EMI instrumental efficiency, and electron detection efficiency (where appropriate), for ν_μ and $\bar{\nu}_\mu$ charged-current events and $\mu^- e^+$ and $\mu^+ e^-$ events are 0.72, 0.78, 0.60, and 0.62, respectively.[23]

The determination of electron momentum is complicated because of bremsstrahlung. A procedure has been developed using the radius of curvature of the electron and measurement of the bremsstrahlung gammas (e^+e^- pairs). The method used to determine the electron momentum is as follows.

(1) The length of track on the film is measured until either the track leaves the chamber, it turns through about 60°, a kink is observed, or a large bremsstrahlung occurs. If necessary a track is further cut back in length until a spiral fit yields a normal rms deviation. This procedure puts an upper limit ($\alpha p_{\text{electron}}$) on the momentum of a bremsstrahlung occurring on all but the beginning of the track. The value of α is approximated by the fractional curvature error of the track.

(2) A helix fit is made to the track and is assumed to give the momentum of the electron at the midpoint of the measured track.

(3) γ's (e^+e^- pairs) within two radiation lengths of the primary vertex and pointing to the primary vertex and with momenta greater than approximately 50 MeV/c are measured. Any γ that is consistent with being tangent to the primary electron at the initial vertex has its momentum added to that of the electron as a bremsstrahlung.

(4) The momentum of the electron is corrected for ionization loss and for undetected low-momentum bremsstrahlung (< 50 MeV) occurring

between the midpoint of the track and the be-
ginning, and for bremsstrahlung γ's with 50 MeV/
$c < p < \alpha p_{\text{electron}}$ which occur beyond the initial
part of the track and before the midpoint of the
track. An average correction is also made for
bremsstrahlung occurring in the initial part of
the track that would not produce a γ $(e^+ e^-)$ in two
radiation lengths. The initial part of the track is
defined as that portion in which the track turns
through an angle equal to twice the angle error.

This method of determining electron momentum
gives a peak at the π^0 mass in $\gamma\gamma$ mass distribu-
tions.

To determine the neutrino energy, the dilepton
events have been fully measured including neutral
interactions, decays, and γ's within two radiation
lengths of the primary vertex. The neutrino en-
ergy E_ν is estimated by summing the momenta
along the neutrino direction. In order to correct
for missing neutrals (including any missing neu-
trinos), we have used an average correction ob-
tained from our dimuon sample using mean trans-
verse-momentum imbalance[10]

$$(P_x^0)_{\text{corr}} = AP_x^0 + B ,$$

where P_x^0 is the sum of the longitudinal momen-
tum of all tracks excluding the muon, $A = 1.28$
± 0.06, and $B = 2.1 \pm 0.6$ GeV/c. This multiplica-
tive correction is somewhat larger for dimuon
events than for normal charged-current events
$(A = 1.16 \pm 0.03; B = 3.3 \pm 0.5$ GeV/$c)$ consistent
with the hypothesis of a missing neutrino. We
use the correction obtained from dimuon events
since the momentum of the muon is better deter-
mined than that of the electron, and we can better
compare the $\mu\mu$ and μe samples if we use the
same correction.[24]

VII. RATES

A. $\mu^- e^+$ events

We have found 8900 neutrino charged-current
events with EMI-identified muons. Of these, 49
contained an e^+ with momentum p_e above 300 MeV/
c. Correcting for backgrounds and losses, elec-
tron scanning efficiency, and detection efficien-
cies, we find

$$R = \text{Rate}(\nu_\mu + N \to \mu^- e^+ X)/\text{Rate}(\nu_\mu + N \to \mu^- X)$$

$$= (0.73 \pm 0.11)\%, \quad p_e > 0.3 \text{ GeV}/c .$$

Removing events with electron momentum below
4 GeV/c, our rate becomes $(0.44 \pm 0.08)\%$, which
may be compared to the $\mu^- \mu^+$ rate of $(0.37 \pm 0.10)\%$
previously reported by this experiment.[10]

To investigate the energy dependence of this
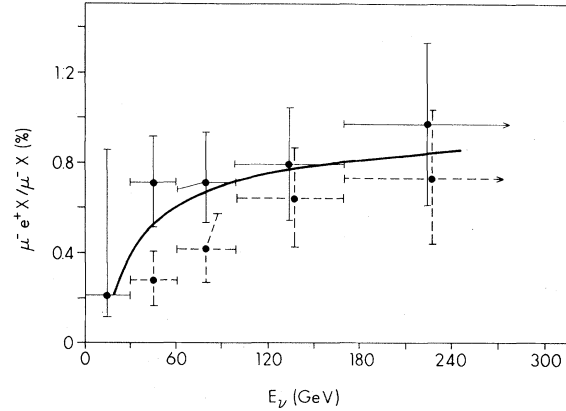ratio, we divide the data into two samples and

FIG. 1. Ratio of $\mu^- e^+ X$ to $\mu^- X$ rates versus ν energy.
The solid error bars are events with $p_e > 0.3$ GeV/c;
the dashed error bars are events with $p_e > 4.0$ GeV/c.
The smooth curve is the charm-excitation curve of Lai[26]
with a semileptonic branching ratio of 0.1.

determine, for $p_e \geqslant 0.3$ GeV/c, $R(E_\nu < 100$ GeV$)$
$= (0.66 \pm 0.13)\%$ and $R(E_\nu > 100$ GeV$) = (0.87$
$\pm 0.21)\%$. Removing events with electron mo-
mentum below 4 GeV/c, we obtain $R(E_\nu < 100$ GeV$)$
$= (0.34 \pm 0.09)\%$ and $R(E > 100$ GeV$) = (0.69 \pm 0.18)\%$,
also in agreement with the dimuon results of this
experiment.[10] The 4-GeV/c requirement intro-
duces a stronger energy dependence of the ratio.
This is shown also in Fig. 1, where we have
divided the data up into finer bins. These results
are summarized along with the dimuon results in
Tables III and IV. They are in reasonable agree-
ment with previous, lower-energy $\mu^- e^+$ results.[1-9]

Of these 49 $\mu^- e^+$ events, four have significant
gaps of 5 to 10 mm in space between the event
vertex and the apparent origin of the e^+ track.
We interpret these gaps as decays of heavy short-
lived particles such as charmed mesons. Further
discussion of these events is presented in Sec. IX.

TABLE III. Dilepton-to-single-lepton ratios (%). The
muon (electron) momentum is required to be greater
than 4 (0.3) GeV/c unless otherwise stated. l_2 refers to
the second lepton.

Ratio	$P_{l_2} > 0.3$ GeV/c	$P_{l_2} > 4.0$ GeV/c
$\mu^- e^+ X/\mu^- X$	0.73 ± 0.11	0.44 ± 0.08
$\mu^- \mu^+ X/\mu^- X$		0.37 ± 0.10
$\mu^+ e^- X/\mu^+ X$	1.1 ± 0.3	0.5 ± 0.2
$\mu^+ \mu^- X/\mu^+ X$		0.5 ± 0.3
$e^- \mu^+ X/e^- X$		$0.7^{+1.1}_{-0.5}$
$e^- e^+ X/e^- X$	$1.0^{+1.0}_{-0.5}$	
$e^+ e^- X/e^+ X$	$1.8^{+3.0}_{-1.1}$	

TABLE IV. Energy dependence of $\mu^- l^+ X/\mu^- X$.

Ratio	l_2 momentum	All E_ν (%)	$E_\nu < 100$ GeV (%)	$E_\nu > 100$ GeV (%)
$\mu^- e^+ X/\mu^- X$	>0.3 GeV/c	0.73 ± 0.11	0.66 ± 0.13	0.87 ± 0.21
$\mu^- e^+ X/\mu^- X$	>4.0 GeV/c	0.44 ± 0.08	0.34 ± 0.09	0.69 ± 0.18
$\mu^- \mu^+ X/\mu^- X$	>4.0 GeV/c	0.37 ± 0.10	0.27 ± 0.13	0.52 ± 0.21

Of particular interest is the strange-particle rate in the dilepton events, since an enhanced rate is expected in the charm model. There are 15 V^0 decays yielding good three-constraint kinematic fits in the 49 $\mu^- e^+$ events: 13 $K_S^0 \to \pi^+ \pi^-$, 1 $\Lambda \to p\pi^-$, and 1 K^0/Λ ambiguity. The fraction of $\mu^- e^+$ events containing a V^0 decay is $(31 \pm 7)\%$ compared to $(11 \pm 2)\%$ for neutrino charged-current events. In order to correct for V^0 detection efficiency, we have weighted V^0 events to account for interactions before decay and for decays too close to the primary vertex (1 cm), outside the bubble chamber, or too close to the bubble-chamber wall (20 cm). V^0's are required to be at least 1 cm from the primary vertex because of the uncertain detection probabilities for V^0's closer than this. We assume 100% scanning efficiency beyond this distance for V^0's in dilepton events. The average V^0 weight for our 15 events is 1.28. Weighting for detection and correcting for unseen decays, we find a ratio

$$(\mu^- e^+ K^0 X)/(\mu^- e^+ X) = 1.1 \pm 0.3 .$$

Treating the K_S^0/Λ ambiguous event as a Λ, the corrected Λ rate becomes

$$(\mu^- e^+ \Lambda X)/(\mu^- e^+ X) = 0.07^{+0.07}_{-0.03} .$$

The combined neutral-strange-particle rate is 1.2 ± 0.3, which may be compared to our dimuon strange-particle rate of 0.6 ± 0.3.[10] To see if the difference between these values could be related to the 4-GeV/c cut in the muon momentum, we have also determined the neutral-strange-particle rate for events with electron momentum greater than 4 GeV/c and find a rate of 1.2 ± 0.4. The difference between the $\mu\mu$ and μe neutral-strange-particle rates is consistent with being statistical. The neutral-strange-particle rates are summarized in Table V, and further discussion of these rates will be found in Sec. VIII C.

B. $\mu^+ e^-$ events

We have identified 1493 antineutrino charged-current events with the EMI. We found 16 events with a μ^+ and an e^- with an expected background due to fake electrons ($p_e > 0.3$ GeV/c) of 1.8 events.

However, we also expect a contribution due to electron neutrino charm production and subsequent decay into a μ^+ and electron neutrino events with fake muons. The separation of events into muon-neutrino- and electron-neutrino-induced events is discussed in Sec. VII D, where the electron-neutrino contamination is found to be $2.1^{+2.3}_{-1.2}$ events.

The dilepton rate correcting for backgrounds and losses, electron scanning efficiency, and detection efficiencies is

$$R = \text{Rate}(\bar{\nu}_\mu + N \to \mu^+ e^- X)/\text{Rate}(\bar{\nu}_\mu + N \to \mu^+ X)$$

$$= (1.1 \pm 0.3)\%, \quad p_e \geq 0.3 \text{ GeV}/c .$$

For electron momentum greater than 0.8 GeV/c, this ratio becomes $(0.8 \pm 0.3)\%$, which is somewhat larger than previous results at lower energies.[5,8] Antineutrinos are expected to produce $\bar{c}$ quarks from $\bar{s}$ quarks in the strange sea so a greater energy dependence of this ratio might be expected in $\bar{\nu}$ events than in ν events where production can take place from both valence and sea quarks. The average energy of our $\bar{\nu}$ dilepton events is 67 GeV. For electron momentum greater than 4.0 GeV/c, the ratio becomes $(0.5 \pm 0.2)\%$, which agrees well with our $\mu^+ \mu^-$ ratio of $(0.5 \pm 0.3)\%$.[10] These results are also summarized in Table III.

Three V^0 decays were found (a K_S^0, a Λ, and a K_S^0/Λ ambiguity), and the corrected neutral-strange-particle rate is

$$(\mu^+ e^- K^0 X + \mu^+ e^- \Lambda X)/(\mu^+ e^- X) = 0.6^{+0.6}_{-0.3}$$

assuming the ambiguous event is a Λ. It is not

TABLE V. Corrected neutral-strange-particle rates (per event).

Sample	K^0	Λ	$K^0 + \Lambda$
$\mu^- e^+ X$	1.1 ± 0.3	$0.07^{+0.07}_{-0.03}$	1.2 ± 0.3
$\mu\mu X$	0.6 ± 0.3	$0.06^{+0.09}_{-0.05}$	0.6 ± 0.3
$\mu^- e^+ X$ and $\mu\mu X$	0.9 ± 0.2	$0.07^{+0.06}_{-0.03}$	1.0 ± 0.2
$\mu^+ e^- X$			$0.6^{+0.6}_{-0.3}$
$\mu^- X$	0.30 ± 0.06	0.08 ± 0.02	0.38 ± 0.07

unexpected to detect Λ's since the spectator s quark can well end up in a Λ. A neutral-strange-particle rate of 1.8 ± 0.7 was found at lower energy.[8]

C. $\mu^- e^-$ and $\mu^+ e^+$ events

Because the background becomes large at low e^- momentum, only $\mu^- e^-$ events with e^- momentum above 0.8 GeV/c were considered. With this cut, the estimated background (corrected for detection efficiency) is 3.6 events. The number of events found was 3. In these events, the e^- momenta were 1.5, 1.6, and 1.5 GeV/c, and no primary neutral strange particles were observed. The observed events are consistent with being all background and lead to a 90%-confidence-level upper limit on the ratio $\mu^- e^- X / \mu^- e^+ X$ of 7% (for $p_e > 0.8$ GeV/c). Another experiment, using 10- and 2-GeV/c momentum requirements on the muon and electron, respectively, has recently reported a ratio of $(16 \pm 8)\%$.[18] With their cuts, we get a 90%-confidence-level upper limit of 4%. If our events are divided into two neutrino-energy bins, the number of events observed ($p_e \geq 0.8$ GeV/c), the background estimate, and the 90%-confidence-level upper limit on the ratio $\mu^- e^- X / \mu^- e^+ X$ are, respectively, 2 events, 1.6 events, and 15% for $E_\nu < 100$ GeV; and 1 event, 2 events, and 12% for $E_\nu > 100$ GeV.

For e^+ momentum greater than 0.3 GeV/c, 1 $\mu^+ e^+$ event was observed, while the estimated background (corrected for detection efficiency) is 0.3 events. These numbers lead to a value for the ratio $\mu^+ e^+ X / \mu^+ e^- X$ ($p_e > 0.3$ GeV/c) of $(7^{+16}_{-6})\%$, with a 90%-confidence-level upper limit of 36%. Although the one event is consistent with background, the e^+ momentum of 6.6 GeV/c is considerably higher than the median value for background events of 0.8 GeV/c. In fact, the background estimate for $p_e > 4$ GeV/c is 0.05 events. The event, which has a neutrino energy greater than 100 GeV, has no observed neutral strange particle.

D. $e^- \mu^+$, $e^- e^+$, and $e^+ e^-$ events

In addition to the ν_μ and $\bar{\nu}_\mu$ interactions produced by the quadrupole triplet beam, we have found approximately 270 ν_e and 70 $\bar{\nu}_e$ interactions. These electron neutrinos, which are produced primarily by K_{e3} decays, should interact the same as ν_μ according to the hypothesis of μ-e universality. An important test of this universality is the production of charmed particles by ν_e. We have searched for dilepton events, $e\mu$ and ee, produced in ν_e interactions and have found two candidates for $e^- \mu^+$, two candidates for $e^- e^+$, and one candidate for
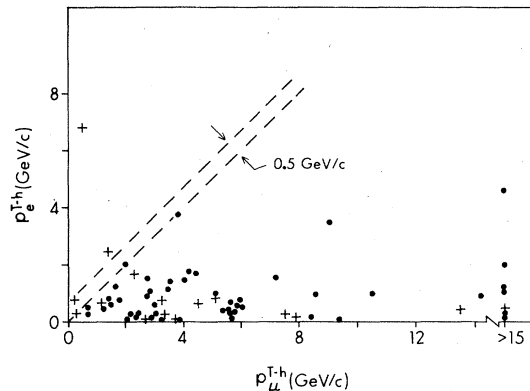

FIG. 2. Plot showing the transverse momentum of the electron versus that of the muon relative to the hadron direction. The hadron direction is determined from the sum of the momenta of all tracks excluding the muon and electron. Dots are for events where the muon is negative, crosses (+) are for events where the muon is positive. The two events above the upper line are taken to be ν_e-induced dilepton events $(e^- \mu^+)$.

$e^+ e^-$.

To separate $e^- \mu^+$ events and $\mu^+ e^-$ events, we have employed a method similar to that which we used to separate $\mu^+ \mu^-$ and $\mu^- \mu^+$ dimuon events,[10] which assumes that all opposite-sign dilepton events involve single charmed particles production. This method is based on the idea that the lepton coming from charm decay will have limited transverse momentum relative to the hadron direction (~ 1 GeV/c), while the primary lepton with a typical large transverse momentum relative to the neutrino direction has an even larger transverse momentum relative to the hadron direction. In Fig. 2, the transverse momentum of the electron versus that of the muon relative to the hadron direction is shown for all μe events, where the hadron direction is determined by the sum of the momenta of all tracks excluding the muon and electron. All events with a μ^- and e^+ have the muon transverse momentum greater than the electron transverse momentum and therefore occur to the right of the diagonal line through the origin. According to the idea above, there are no clear candidates for $e^+ \mu^-$ events. The events with a μ^+ and an e^- have a few events to the left of this line and have two events to the left of the diagonal line displaced 0.5 GeV/c to the left of the line through the origin. Since we observe many more ν_e interactions than $\bar{\nu}_e$ interactions, we would expect to find more $e^- \mu^+$ events than $e^+ \mu^-$ events. We have used our charm production and decay Monte Carlo (described below) to estimate the separation of events about the leftmost diagonal line. For a muon momentum greater than 4 GeV/

TABLE VI. Electron-neutrino dilepton events. E and p_l^{T-h} are the lepton energy and momentum transverse to the hadron direction, respectively. Φ_h is the angle between the electron and hadron direction in the plane perpendicular to the neutrino direction. E_ν is the corrected event energy, and x and y are the usual scaling variables.

Event	Type $(l_1 l_2)$	$p_{l_1}^{T-h}$ (GeV/c)	$p_{l_2}^{T-h}$ (GeV/c)	E_{l_1} (GeV)	E_{l_2} (GeV)	Φ_h (deg)	E_ν (GeV)	x	y
14 851 214	$e^- \mu^+$	6.8	0.52	57.1	8.2	178	130	0.22	0.56
16 381 805	$e^- \mu^+$	2.5	1.40	9.9	26.4	175	62	0.23	0.85
15 581 662	$e^- e^+$	2.7	0.19	20.3	2.3	170	87	0.17	0.78
16 030 177	$e^- e^+$	3.5	0.94	39.6	3.2	131	63	0.12	0.38
15 270 192	$e^+ e^-$	6.3	0.25	50.0	4.4	161	94	0.17	0.47

c, the Monte Carlo program predicts that 86% of $e^- \mu^+$ events will occur to the left of this line, while only 1.4% of $\mu^+ e^-$ events will occur there. Assuming that electron neutrino events with a false muon will separate in a similar fashion, we can break up our 16 events into the following classifications: 13.9 events $\bar{\nu}_\mu$-induced (12.5 $\mu^+ e^-$, 1.4 background) and 2.1 events ν_e-induced (1.6 $e^- \mu^+$, 0.5 background).

Table VI lists identification and kinematic quantities for the two $e^- \mu^+$ events. A further indication that these two candidates come from ν_e interactions is given by their Φ_h angles. This angle is the angle between the electron momentum and the total hadron momentum in the plane perpendicular to the neutrino direction. The two $e^- \mu^+$ candidates have Φ_h approximately 180°, characteristic of ν_e interactions.

The muon background for $e^- \mu^+$ is 0.5 events (including detection efficiency), due largely to $\pi^+ \to \mu^+$ decay. The rate corrected for background and acceptance is

$$R = \text{Rate}(\nu_e + N \to e^- \mu^+ X)/\text{Rate}(\nu_e + N \to e^- X)$$

$$= (0.7^{+1.1}_{-0.5})\%.$$

We have also found three events with an e^+ and an e^-. We require the $e^+ e^-$ invariant mass to be greater than 0.8 GeV/c^2 in order to eliminate η Dalitz decays (also ρ and ω decays). Based on transverse momentum relative to the hadron direction, two of the events appear to be ν_e induced and one appears to be $\bar{\nu}_e$ induced. The properties of these events are also presented in Table VI. The rates corrected for background, acceptance, and the $e^+ e^-$ invariant mass cut for these events are

$$R = \text{Rate}(\nu_e + N \to e^- e^+ X)/\text{Rate}(\nu_e + N \to e^- X)$$

$$= (1.0^{+1.0}_{-0.5})\%,$$

$$R = \text{Rate}(\bar{\nu}_e + N \to e^+ e^- X)/\text{Rate}(\bar{\nu}_e + N \to e^+ X)$$

$$= (1.8^{+3.0}_{-1.1})\%.$$

These rates are given in Table III and are in agreement with our $\mu \mu$ and μe rates. No primary neutral strange particles were detected in the ν_e or $\bar{\nu}_e$ induced events.

We believe these events constitute the first evidence for charm production by *electron* neutrinos.

E. Multilepton events

No trilepton events ($\mu \mu \mu$, $\mu \mu e$, $\mu e e$, or eee in any charge combination) were found with $p_\mu > 4$ GeV/c, $p_e > 0.3$ GeV/c, and mass of any $e^+ e^-$ combination greater than 0.8 GeV/c^2.

One event was found with four outgoing leptons and a visible K_s^0 decay, $\mu^+ e^- e^+ e^- K_s^0$. The kinematics of this event make it probable that it originated from a muon antineutrino. More details can be found in a previous publication.[25]

VIII. COMPARISON WITH CHARM MODEL

In the previous section, we determined the amount of dilepton production in various channels. In this section, we wish to examine the details of the μe dilepton events and compare the events with what would be expected under the hypothesis of charm production and semileptonic decay.

A. Monte Carlo program

We have written a Monte Carlo program originally based on that of Lai[26] but extended to include other decay models. In the Monte Carlo calculation, charmed quarks (c) are produced by neutrinos from d quarks (rate $\propto \sin^2 \theta_c$) and s quarks (rate $\propto \cos^2 \theta_c$), and $\bar{c}$ quarks are produced by antineutrinos from $\bar{s}$ quarks (rate $\propto \cos^2 \theta_c$). Any mixing with a third quark doublet is neglected. The helicities involved in these couplings imply uniform y distributions ($y = \nu/E_\nu$, $\nu = E_\nu - E_\mu$) for both neutrinos and antineutrinos. Thresholds and experimental cuts, of course, modify this. Scaling is assumed to hold, and the Field-Feynman parametrizations[27] are used to describe the momen-

tum distributions of quarks in the nucleon. However, to account for the mass corrections in the light-to-heavy-quark transition, a rescaling variable is introduced[28]

$$\xi = x + m_c^2/(2M_n E_\nu y) \, ,$$

where m_c is the effective mass of the charmed quark (taken to be 1.5 GeV/c^2 in Lai's model), M_n is the nucleon mass, and x is the usual scaling variable $(x = Q^2/2M_n\nu)$.

After production, the charmed quark fragments into a charmed hadron, which carries a fraction z of the original charmed-quark energy. Although fragmentation functions for light quarks decrease rapidly with z, as $z^{-1}(1-z)$, the fragmentation function for a charmed quark may have little or no z dependence.[26] Our dimuon events are well represented by a uniform z distribution,[10] and we use this distribution here (unless otherwise noted) for comparison with our μe events. The charmed hadron is given a transverse momentum (p_t) relative to the direction of the charmed quark according to the distribution

$$dN/dp_t^2 = \exp[-6(p_t^2 + m_c^2)^{1/2}] \, .$$

Finally the charmed hadron is allowed to decay. Earlier, for comparison with the dimuon sample,[10] we used only the model of Lai,[26] which treats the decay process approximately by the quark decay reactions

$$c \rightarrow s l^+ \nu_l \, ,$$

$$\bar{c} \rightarrow \bar{s} l^- \bar{\nu}_l \, ,$$

where the Cabibbo-suppressed modes are ignored. Now we also use a second model,[29] where we form D mesons and allow them to decay one-half of the time by $D \rightarrow \bar{K} e \nu$ and the other half by $D \rightarrow \bar{K}^* e \nu.$[30] Even if $\bar{K}^*$ production is not this frequent, the latter decay will simulate nonresonant multihadron decay approximately. The second model gives nearly identical results to the first model in most instances. To avoid confusion on the plots, only the Lai-model prediction is shown when the two models are nearly identical. The same lepton-momentum cuts are applied to the Monte Carlo events as to real dilepton events.

B. Comparison with data

In Fig. 3 we present the energy distributions of the muons in the $\mu^- e^+$ and $\mu^+ e^-$ events along with the predicted distributions from the Monte Carlo. The events have been weighted to correct for both electron and muon detection efficiencies. In Fig. 4 we show the corrected-electron-energy distributions. The average value of the muon momentum divided by the average value of the elec-
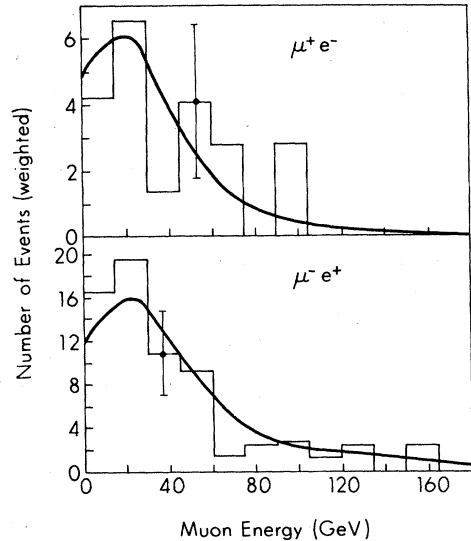

FIG. 3. Number of events (weighted) versus the muon energy E_μ in $\mu^- e^+$ and $\mu^+ e^-$ events. The events have been weighted for EMI and electron detection efficiency. In Figs. 3-17, the solid smooth curves are the Monte Carlo predictions using Lai's (quark-decay) model with a constant fragmentation function; the dashed smooth curves are the Monte Carlo prediction using 50% $D \rightarrow \bar{K} e \nu$ and 50% $D \rightarrow \bar{K}^* e \nu$. If the predictions of the two models are nearly the same, then only Lai's model is shown.

tron momentum in $\mu^- e^+$ $(\mu^+ e^-)$ events is 5.2 ± 1.0 (8.9 ± 3.0), indicating that the events are inconsistent with being predominantly heavy lepton production and decay.[31] Figure 5 shows the corrected-neutrino-energy distributions. The anti-
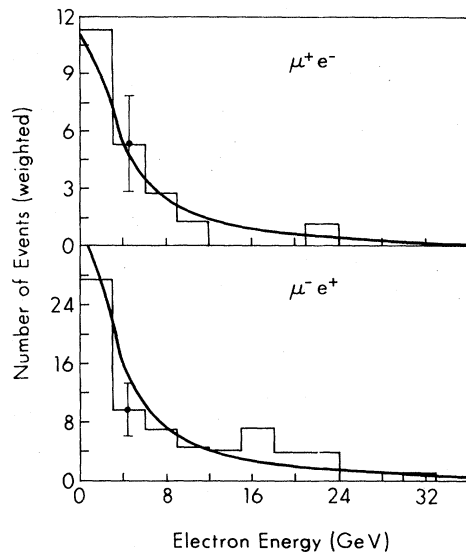

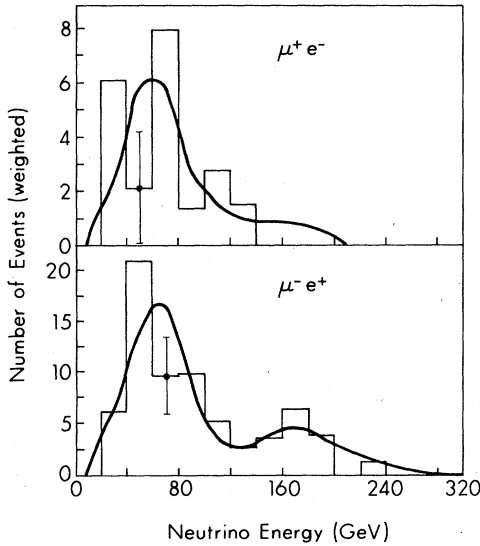FIG. 4. Number of events (weighted) versus corrected electron energy E_e. For more detail, see caption of Fig. 3.

FIG. 5. Number of events (weighted) versus corrected neutrino energy E_ν. For more detail, see caption of Fig. 3.

neutrino energy spectrum is softer than the neutrino spectrum, and this is reflected in the electron and muon energy distributions also. The average energies of the μ^-e^+ and μ^+e^- events are 91 and 67 GeV, respectively. In Fig. 6 the distributions in Φ_e, which is the angle between the muon and the electron in the plane perpendicular to the neutrino, are shown. The events occur predominantly at large Φ_e, in agreement with the Monte Carlo and supporting the interpretation that
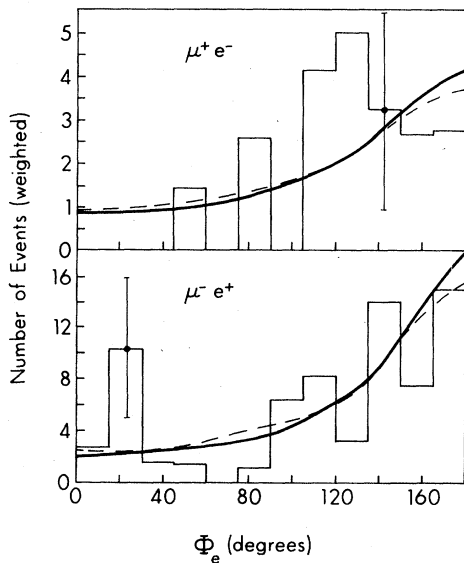
FIG. 6. Number of events (weighted) versus Φ_e, the angle between the muon and electron in the plane perpendicular to the neutrino direction. See caption of Fig. 3.
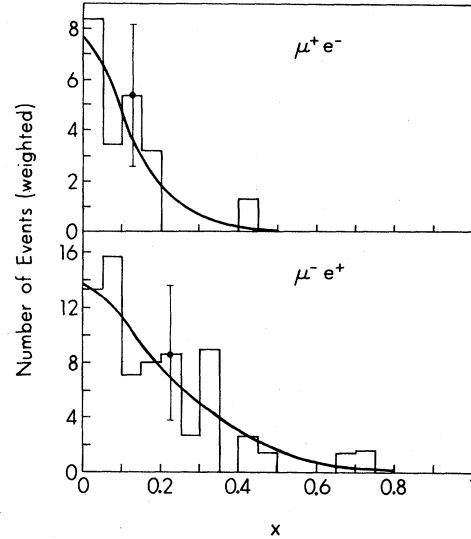
FIG. 7. Number of events (weighted) versus x. $x = Q^2/2M_n \nu$, where Q^2 is the four-momentum transfer squared, M_n is the nucleon mass, and $\nu = E_\nu - E_\mu$. See caption of Fig. 3.

the origin of the electrons is hadronic. Figures 7–11 present x, y, Q^2 (four-momentum transfer squared), W (invariant mass of the hadron system), and $p_\mu^{T-\nu}$ (muon transverse momentum relative to the neutrino direction) distributions, respectively. As expected, the x distribution is broader for μ^-e^+ events ($\bar{x} = 0.19 \pm 0.02$) than for μ^+e^- events ($\bar{x} = 0.10 \pm 0.03$) since in the former case charm may be produced from valence quarks as well as sea quarks.
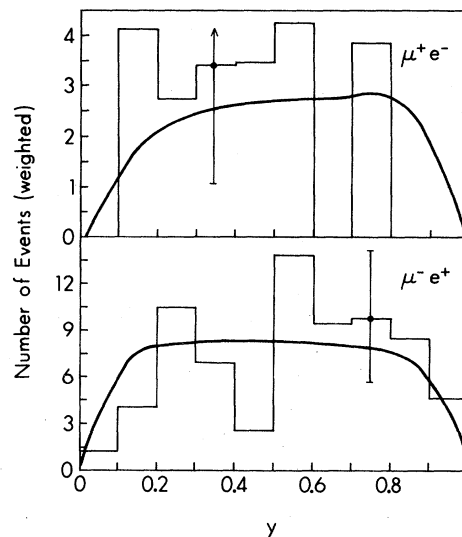
In Fig. 10 there appears to be an excess of

FIG. 8. Number of events (weighted) versus y, where $y = \nu/E_\nu$. See caption of Fig. 3.
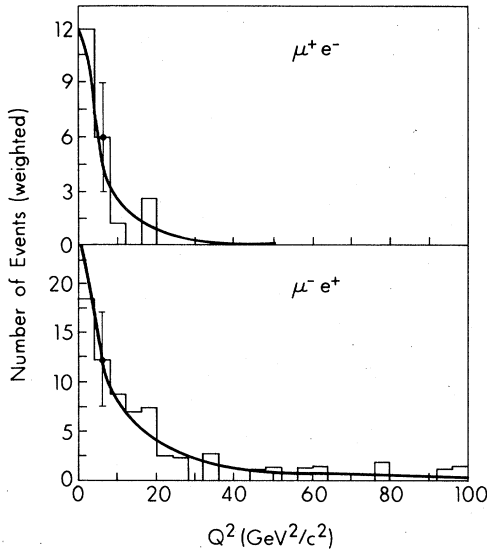
FIG. 9. Number of events (weighted) versus Q^2, the four-momentum transfer squared. See caption of Fig. 3.

$\mu^+ e^-$ events with $W \sim 5$ GeV/c^2 compared to the prediction. Recently Armenise et al.[12] reported a peak near 6 GeV/c^2 in W which is correlated to a peak near 1.15 GeV/c in $p_\mu^{T-\nu}$ of the μ^+ in $\bar{\nu}$-produced dimuon events. They suggest that quasi-elastic two-body B-baryon production might explain part of the excess in W, however they find that such a model does not predict a peak in $p_\mu^{T-\nu}$. Our $\bar{\nu}$-induced dimuon events also hint of an excess in W, albeit with poor statistics. Combining our 14 $\mu^+ e^-$ and 5 $\mu^+ \mu^-$ events, we find 9 events with $5 < W < 6.5$ GeV/c^2. Our charm-decay
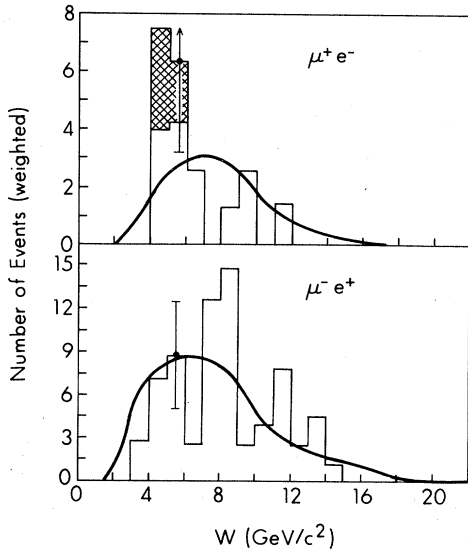
FIG. 10. Number of events (weighted) versus W, the invariant mass of the hadron system. See Fig. 3 caption. The cross-hatched events have $p_e < 0.8$ GeV/c.
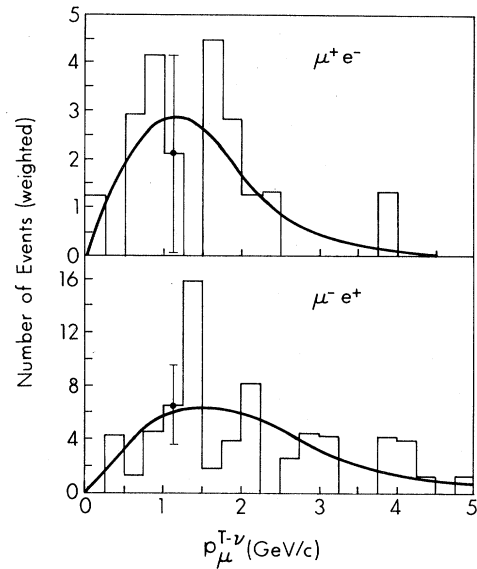
FIG. 11. Number of events (weighted) versus the transverse momentum of the muon relative to the neutrino direction. See Fig. 3 caption.

model normalized to 19 events and including $\mu^+ \mu^-$ background predicts 3.5 events in the range $5 < W < 6.5$ GeV/c^2. However, our $\mu^+ e^-$ events do not show a strong deviation from the charm model in other distributions that we have looked at. We also note that the correlation of Armenise et al.[12] between the W peak and $p_\mu^{T-\nu}$ of the μ^+ is not present in our $\mu^+ e^-$ (nor $\mu^+ \mu^-$) events (see Fig. 11).

The distributions of momenta perpendicular to the μ-ν plane of the electrons and V^0's are shown in Figs. 12 and 13, respectively.[32] The Monte Carlo events are weighted to account for loss of V^0's by interaction before decay and loss of decays within one cm of the primary vertex, outside the bubble chamber, and within 20 cm of the bubble-chamber wall. The Monte Carlo predicts distributions for kaons from charmed-particle decay only. Strange particles from associated production and spectator strange quarks are not accounted for. One must take this into consideration when comparing V^0 Monte Carlo distributions with the data. For completeness, we show the V^0 distributions for the $\mu^+ e^-$ events as well as the $\mu^- e^+$ events. The Λ's are shaded in the V^0 distributions.

Figures 14 and 15 show the z distributions ($z_e = E_e / \nu$ and $z_V = E_V / \nu$) for electrons and V^0's, respectively. These distributions do not measure the fragmentation function of the c quark directly since the electron and V^0 are only decay products of the charmed hadron and therefore carry only part of the energy. However, they are quite sensitive to the form of the fragmentation function. Al-
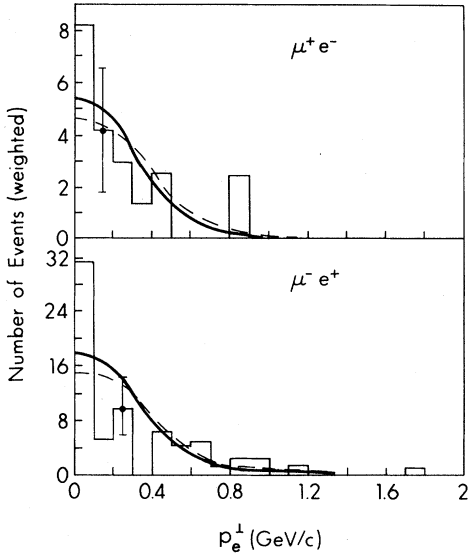
FIG. 12. Number of events (weighted) versus the momentum of the electron perpendicular to the plane formed by the neutrino and muon. See Fig. 3 caption.

so shown in these figures are the Monte Carlo predictions for $z^{-1}(1-z)$ and $z(1+z)$ fragmentation functions, as well as those for the uniform fragmentation function. For a more complete discussion of fragmentation models, see Ref. 26. The z_e and z_V distributions are consistent with the Monte Carlo model using the uniform fragmentation function.

Another variable which is useful in the study of fragmenting quarks is the rapidity of the particle
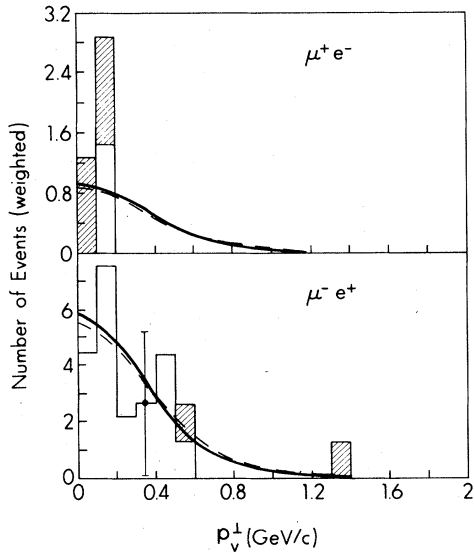
FIG. 13. Number of V^0 events (weighted) versus the V^0 momentum perpendicular to the μ-ν plane. See caption of Fig. 3. The shaded events are Λ's.
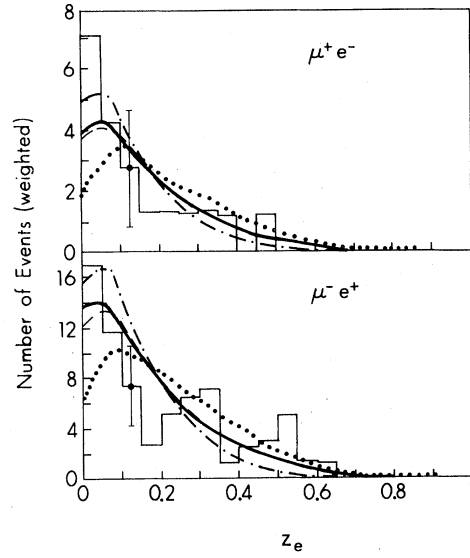

FIG. 14. Number of events (weighted) versus z_e, $z_e = E_e/\nu$. See Fig. 3 caption. In this figure and in Figs. 15–17, we also show the Monte Carlo predictions for a $z^{-1}(1-z)$ fragmentation function (dashed-dotted curve) and for a $z(1+z)$ fragmentation function (dotted curve).

in the quark's rest frame.[33] We define[33] this in general as

$$Y_q = Y_{\mathrm{lab}} - \ln(W^2/M_n^2),$$

where

$$Y_{\mathrm{lab}} = 0.5 \ln[(E+p_{\shortparallel})/(E-p_{\shortparallel})]$$

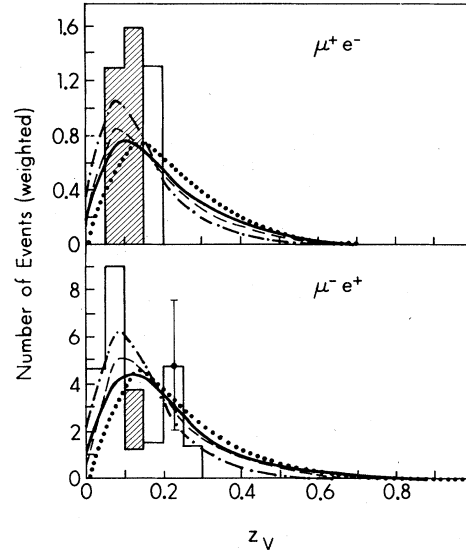for each particle and where E is the particle en-

FIG. 15. Number of V^0 events (weighted) versus z_V, $z_V = E_V/\nu$. The smooth curves are described in the captions of Figs. 3 and 14. Shaded events are Λ's.
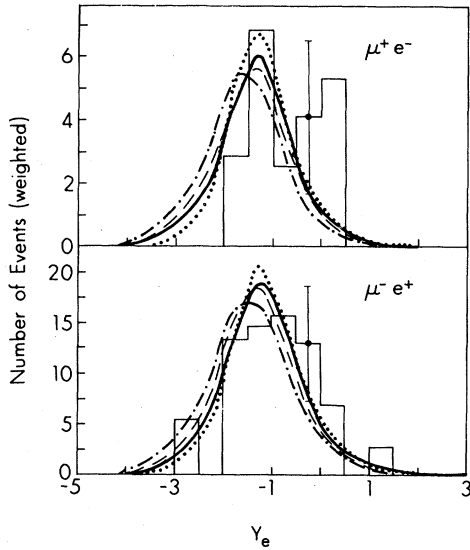
FIG. 16. Number of events (weighted) versus the rap-
idity of the electron Y_e. The smooth curves are de-
scribed in the captions of Figs. 3 and 14.

ergy and $p_{\parallel}$ is the momentum parallel to the
hadron direction. In Figs. 16–19, the rapidity
distributions of the electrons, V^0's, positive
hadrons, and negative hadrons are shown, respec-
tively.

In Fig. 20 we show the e-V^0 invariant-mass dis-
tributions for our μe events combined with the
μ-V^0 invariant-mass distributions for our dimuon
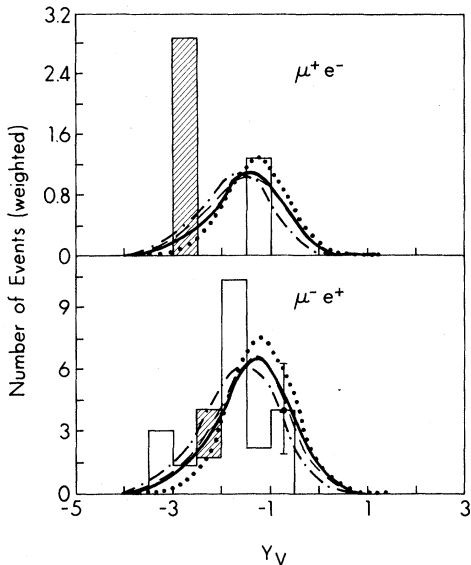events. On this figure, we show also the predicted

FIG. 17. Number of V^0 events (weighted) versus the
V^0 rapidity, Y_V. The smooth curves are described in the
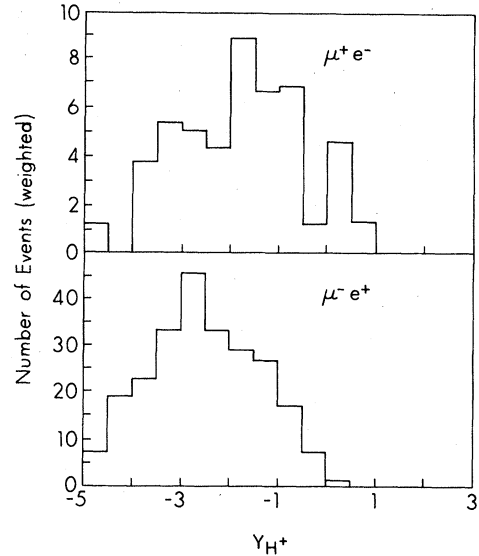captions of Figs. 3 and 14. Shaded events are Λ's.

FIG. 18. Number of events (weighted) versus the rap-
idity of the positive hadrons.

distributions for pure $D \to \bar{K}l\nu$ and $D \to \bar{K}^*l\nu$. The
μ^-e^+ data fit $D \to \bar{K}^*l\nu$ poorly but are consistent
with either pure $D \to \bar{K}l\nu$ or the model which uses
50% $D \to \bar{K}l\nu$ and 50% $D \to \bar{K}^*l\nu$. The quark decay
model of Lai does not fit well either, but this is
partially explained by the fact that this model
uses the bare quark mass of 1.5 GeV/c^2 rather
than the D mass.

In all of the figures, the agreement between the
Monte Carlo distributions using 50% $D \to \bar{K}e\nu$ and
50% $D \to \bar{K}^*e\nu$ and our data is good, except pos-
sibly for the W distribution for μ^+e^- events. This
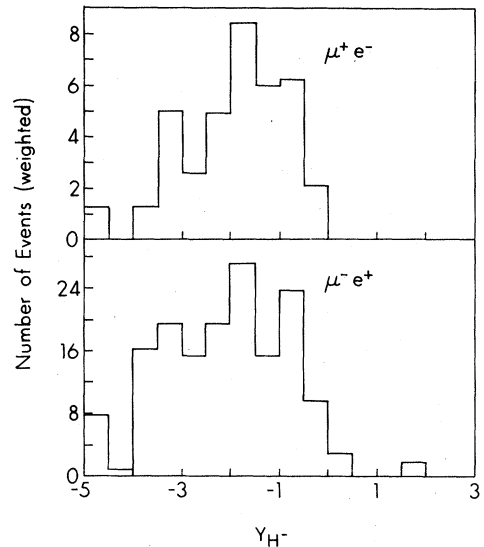is demonstrated also in Table VII, where we

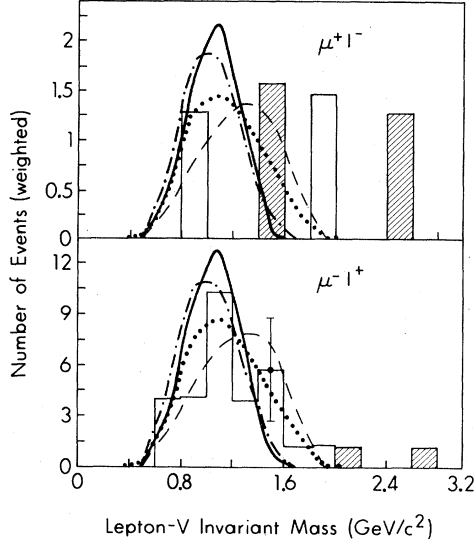FIG. 19. Number of events (weighted) versus the rap-
idity of the negative hadrons.

FIG. 20. Number of V^0 events (weighted) versus the lepton-V^0 invariant mass using the combined μe and $\mu\mu$ samples. The smooth curves shown are the Monte Carlo predictions of Lai's quark-decay model (solid curve), $D \rightarrow \bar{K}e\nu$ (dashed curve), $D \rightarrow \bar{K}^*e\nu$ (dash-dotted curve), and 50% $D \rightarrow \bar{K}e\nu$ and 50% $D \rightarrow \bar{K}^*e\nu$ (dotted curve).

present the means of the distributions shown in the figures and those predicted by the Monte Carlo distributions.

C. K^* search

We have also searched for direct evidence of K^* production in our μ^-e^+ and $\mu^-\mu^+$ events. When a charmed particle decays, an s quark is expected in the Cabibbo-favored decay. This should lead to final states with negative strangeness, so any K^*'s should appear in states with K^- and $\bar{K}^0$ but not with K^+ or K^0. We have plotted all possible $K\pi$ mass combinations where the $K\pi l$ invariant mass is less than the D mass. The $K^-\pi^+$ and $K^+\pi^-$ mass combinations are shown in Fig. 21. Since charged kaons are not usually identified in the bubble chamber, all tracks that are not uniquely identified as something else are plotted in the invariant-mass plot as possible kaons. No strong peak is seen in the region of the K^* on either plot. The excess of events at around 1.1 GeV/c^2 in the $K^-\pi^+$ distribution in Fig. 21 corresponds to no known resonance and appears to originate from multiple combinations from a

TABLE VII. Comparison of mean values for μe events and Monte Carlo (MC) events using a model with 50% $D \rightarrow \bar{K}e\nu$ and 50% $D \rightarrow \bar{K}^*e\nu$ and a uniform fragmentation function. Monte Carlo predictions marked with an asterisk do not include contributions from spectator strange quarks or from associated production.

| Variable	μ^-e^+ Data	μ^-e^+ MC	μ^+e^- Data	μ^+e^- MC
E_μ (GeV)	41.7 ±5.5	47	42 ±8	35
E_e (GeV)	8.2 ±1.1	6.9	4.7 ±1.3	6.3
E_ν (GeV)	91 ±7	95	67 ±8	75
Φ_e (deg)	115 ±8	122	125 ±8	114
x	0.19 ±0.02	0.19	0.10 ±0.03	0.11
y	0.55 ±0.03	0.49	0.42 ±0.05	0.53
Q^2 (GeV^2/c^2)	18.8 ±2.5	15.3	5.5 ±1.3	8.0
W (GeV/c^2)	8.3 ±0.4	7.8	6.3 ±0.6	7.7
$p_\mu^{T\cdot\nu}$ (GeV/c)	2.1 ±0.2	2.0	1.5 ±0.2	1.5
$p_e^\perp$ (GeV/c)	0.32 ±0.05	0.29	0.25 ±0.07	0.29
$p_\nu^\perp$ (GeV/c)	0.31 ±0.07	0.31*	0.12 ±0.03	0.30*
z_e	0.21 ±0.02	0.18	0.15 ±0.04	0.18
z_ν	0.12 ±0.02	0.18*	0.13 ±0.02	0.18*
Y_e	−0.94 ±0.12	−1.3	−0.70 ±0.18	−1.4
Y_ν	−1.9 ±0.2	−1.5*	−2.3 ±0.4	−1.6*
$M_{\text{lepton} - V^0}$ (GeV/c^2)	1.27 ±0.05	1.14*	1.7 ±0.3	1.14*
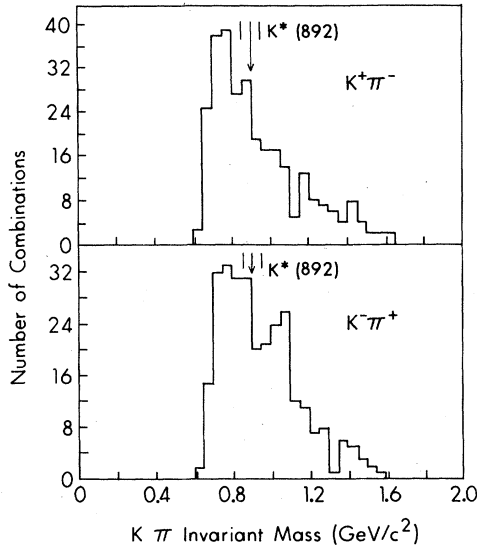
FIG. 21. Invariant-mass combinations of $K^+\pi^-$ and $K^-\pi^+$ for $\mu^-\mu^+$ and μ^-e^+ dilepton events. Only those combinations are plotted where the $K\pi$ –lepton invariant mass is less than the D mass. No strong peak is seen in the region of the K^*.

few high-multiplicity events. Using the $K^+\pi^-$ mass plot to estimate background under the $K^-\pi^+$ mass plot, we estimate 8 ± 14 $\bar{K}^* \rightarrow K^-\pi^+$ events. No strong evidence for K^*'s is seen on any other mass plot.

We have attempted to estimate how many $\bar{K}^*$'s we might expect to see assuming that all production is due to D decay and that D decay proceeds 50% of the time through $D \rightarrow \bar{K}^*e\nu$. Recent direct charmed-particle lifetime measurements made in a Fermilab ν emulsion experiment[34] and semileptonic-branching-ratio measurements obtained at SPEAR[35] indicate that the D^+ semileptonic branching ratio is much greater than the D^0 ratio. There is also evidence in the emulsion experiment[34] and in a BEBC experiment[36] that production of D^*'s, which decay into $D\pi$, is quite important in charm production by neutrinos. We therefore assume that D^+'s and D^0's are produced in equal numbers and that D^{*+}'s and D^{*0}'s are produced in equal numbers and calculate the $\bar{K}^*$ production, as a function of the fraction of the final D's which are due to D^* production. Using these assumptions, the D^* branching ratios,[37] the D^+ and D^0 semileptonic branching ratios (taken to be 0.2 and 0.02, respectively),[34] the K^* branching ratios into final $K\pi$ states, and efficiencies for detecting K^0's and π^0's, we estimate that the number of $K^-\pi^+$, $K^0_S\pi^0$, $K^-\pi^0$, and $K^0_S\pi^-$ events detected should be, respectively, 24, 2, 0.6, and 0.8 for no D^* production; 22, 1.8, 1.1, and 1.5 for 50% D^* production; and 17.6, 1.5, 2.2, and 2.9 for 100% D^*

production. We are most sensitive to the $K^-\pi^+$ state, and the number of $K^-\pi^+$ events expected from $\bar{K}^*$ production varies slowly with the fraction of D^* production. Clearly we cannot rule out (or confirm) $D \rightarrow \bar{K}^*e\nu$ occurring 50% of the time.

D. Neutral-strange-particle rates in ν_μ dilepton events

The neutral-strange-particle rates for μ^-e^+ events were determined in Sec. VII A and are summarized in Table V. The combined $(K^0+\Lambda)$ rate is 1.2 ± 0.3. Assuming that strange-particle production is the same in μ^-e^+ and $\mu^-\mu^+$ events, we obtain a combined neutral-strange-particle rate for the overall sample of 1.0 ± 0.2. We emphasize that most of the V^0's are K^0_S's. Combining the μ^-e^+ and $\mu^-\mu^+$ events, we have 20 K^0_S's, 3 Λ's, and 1 K^0_S/Λ ambiguity (which we count as a Λ in rate determinations). The Λ rate in ν-induced dilepton events is the same as that in ν charged-current events.

Recently, the BNL-Columbia experiment[18] reported dilepton neutral-strange-particle results in terms of the excess number of strange particles over that expected in charged-current (CC) interactions. A comparison in terms of this excess, which is just the difference between the neutral-strange-particle rate in dilepton events and that in CC events, is better than comparing total strange-particle rates since our experiment is at higher energy and finds an increased neutral-strange-particle rate in CC interactions compared to the BNL-Columbia experiment. However, this difference is not a proper measure of the strange-particle contribution due to charm in dilepton events since the CC neutral-strange-particle rate includes a contribution due to charm (see below). The BNL-Columbia experiment finds a difference of 0.6 ± 0.15 neutral-strange particles per μ^-e^+ event,[18] which is in good agreement with our difference of 0.8 ± 0.3 (μ^-e^+ only) or 0.6 ± 0.2 (μ^-e^+ and $\mu\mu$) neutral-strange particles per event. However, they find a difference of 0.11 ± 0.04 Λ^0's per event compared to our value of $-0.01^{+0.07}_{-0.04}$ (μ^-e^+ only) or $-0.01^{+0.06}_{-0.04}$ (μ^-e^+ and $\mu\mu$) Λ^0's per event, although the disagreement is only 1.7σ.

The second lepton-Λ invariant masses are 2.14, 7.0, 2.63, and 3.28 GeV/c^2 (for the Λ/K ambiguity). Only one of these (a μ^-e^+ event) is consistent with being a Λ^+_c decay. However, Λ^+_c production has been observed in ν interactions.[34,38,39] The $\Lambda^+_c \rightarrow \Lambda\pi^+$ and $\Lambda^+_c \rightarrow \bar{K}p$ signals seen in a neutrino-deuterium experiment,[39] when combined with upper limits on the Λ^+_c branching ratios into these modes taken from an e^+e^- experiment,[40] imply a lower limit on the ratio $(\nu D \rightarrow \mu^-\Lambda^+_c X)/(\nu D \rightarrow \mu^-X)$ of 5%.

If the fraction of Λ_c^+ produced in our experiment is 5% (we note that deuterium is an isoscalar target and our neon-hydrogen mixture is nearly an isoscalar target and that the deuterium experiment's mean neutrino energy was 50 GeV, somewhat lower than ours), then the one possible $\Lambda_c^+ \to \Lambda e^+ X$ decay observed here leads to a 90%-confidence-level upper limit on the Λ_c^+ branching ratio into $\Lambda e^+ X$ of 2.2%. We do not give an upper limit for $\Lambda \mu^+ X$ because of the uncertain correction for the 4 GeV/c cut in muon momentum.

The different D^+ and D^0 semileptonic branching ratios (see previous section) also alter the number of neutral strange particles expected; the naive assumption that semileptonic D decays will give an average of 0.5 K^0's per decay is incorrect. For example, if all the decays are via $D^+ \to \bar{K}^0 e^+ \nu$, then we would expect 1 $\bar{K}^0$ per decay. If all the events are due to D^+ decay and if 50% of the decays are $D \to \bar{K}^* e\nu$, then we would expect 0.67 $\bar{K}^0$'s per decay. Finally, using the assumptions of the previous section, we estimate the number of $\bar{K}^0$'s/decay to be 0.64 if there are no D^*'s; 0.61 for 50% D^* production; and 0.56 for 100% D^* production. The ratio varies slowly with the fraction of D^* production. Also, the ratio decreases by only 0.03 if the ratio of the D^+ and D^0 semileptonic branching ratios is decreased by a factor of two. In addition, we would get neutral-strange particles from spectator quarks and from associated production. Using a determination that approximately 40% of ν-produced dilepton events are from strange sea quarks,[41] we expect approximately 0.4 strange particles per dilepton event from spectator $\bar{s}$ quarks and assume that half of these will be neutral.

To determine the neutral-strange-particle associated-production contribution in our ν dilepton events, we make the following assumptions: (1) the unassociated production contribution to the strange-particle rate in noncharm CC events is negligible, (2) 10% of CC events are from charm, (3) the number of decay and spectator strange particles in charm events is 1.4/event, (4) 50% of these will be neutral, and (5) associated production in dilepton events will be the same as that in our noncharm CC events. Correcting for the charm contribution using the above assumptions lowers the CC neutral-strange-particle rate from 0.38/event (see Table V) to 0.31/event. The predicted dilepton neutral-strange-particle rate, including the contribution from charm decay, from the spectator $\bar{s}$ quark, and from associated production under the above assumptions, is 1.1 neutral strange particles per event. This is consistent with our experimental value ($\mu^-\mu^+$ and μ^-e^+) of 1.0 ± 0.2 neutral strange particles per event.

IX. CHARM-LIFETIME DETERMINATION

As mentioned in Sec. VIII, examination of our sample of dilepton events revealed four events where the semileptonic decay of a short-lived particle was directly observed. These events are described in a previous publication.[42] The neutral decays (events $N1$ and $N2$) are consistent with being D^0 decays; the charged decay (event $C1$) is consistent with being a D^+ decay. The charge of the decaying particle is undetermined in the fourth event ($U1$). Because of the undetected neutrino from the semileptonic decay, we cannot conclusively identify the decaying particles but it is quite plausible that they are D mesons. Another likely dilepton event ($C2$) was found but is not included in our sample because of inadequate muon identification. This event has a one-prong charged decay yielding a 3 GeV e^+.

These observed decays together with the dilepton events in which the decays are unseen allow one to determine the lifetimes of the decaying particles. The unseen decays effectively determine the upper limits and the seen decays determine the lower limits on the lifetimes. Our severe experimental bias against observation of close decays can be accounted for using the maximum-likelihood technique. We performed such an analysis previously.[42] We update the lifetimes determination here because we now have more μ^-e^+ events and because new data suggests that the numbers of D^0 and D^+ in the μ^-e^+ and $\mu^-\mu^+$ samples may be significantly different from what we had assumed.

Because the D^0 and D^+ may have significantly different lifetimes, we attempt to determine the D^0 and D^+ lifetimes separately by maximizing the likelihood functions that express the products of the probabilities (P_S) for the seen decays and the probabilities (P_U) for not detecting decays in events where none are seen. For this determination, events $N2$ and $U1$, with their somewhat uncertain decay distances, are treated as unseen decays. The probabilities are given by

$$P_S = e^{-l/\eta c \tau}/\eta c \tau,$$

$$P_U = P_B + (1 - P_B)[P_{D^0}(1 - e^{-l_{\max}/\eta c \tau}) + (1 - P_{D^0})]$$
$$\text{for } D^0 \text{ decays},$$

$$P_U = P_B + (1 - P_B)\{P_{D^+}[P_1 + (1 - P_1)(1 - e^{-l_{\max}/\eta c \tau})]$$
$$+ (1 - P_{D^+})\} \text{ for } D^+ \text{ decays},$$

where

$\eta = $ estimated D momentum divided by D mass,
$\tau = D$ lifetime (either τ_{D^0} or τ_{D^+} where appropriate),
$l = $ decay distance for observed decays,

l_{max} = maximum decay distance for an unseen decay,

P_B = probability that the event is background (has no charmed particles),

P_{D^0} = fraction of dilepton events having a D^0,

P_{D^+} = fraction of dilepton events having a D^+,

and

P_1 = probability that the D^+ decays to only one charged particle (such decays are assumed to be undetectable).

We take $P_B = 0.35$ for dimuon and $P_B = 0$ for μe events. The probability P_1 is taken to be $\frac{2}{3}$; the upper limits for the D^+ lifetime are reduced somewhat for values less than $\frac{2}{3}$. Our previous analysis assumed $P_{D^0} = P_{D^+} = 0.5$—that is, we assumed that all dilepton events resulted from D^0 or D^+ decays and that the relative numbers of D^0 and D^+ semileptonic decays were equal. We now discard the latter assumption and calculate life-times for a range of P_{D^0} (equals $1 - P_{D^+}$) values. As noted earlier in this paper, deviations from the naive $P_{D^0} = 0.5$ value can result from D^* production and from unequal D^+ and D^0 semileptonic branching ratios.

Two major problems in this analysis are esti-mating l_{max} and the D momentum for each event with an undetected decay. The distance l_{max} is obtained by judging how far from the primary vertex a neutral decay into two charged particles or a charged decay into three charged particles would have to occur in order that it is evident that not all tracks originate at the primary vertex. The median value of l_{max} for our 86 events is 1.5 cm. The D momentum spectrum from our dilep-ton Monte Carlo is used to estimate average values for the exponential terms in the probabil-ities P_S and P_U. The averages are calculated by integrating over the D spectrum starting from the momentum of the lepton for the unseen decays and from minimum D momentum for the seen decays. The results from this technique are similar to those obtained by taking the D momen-tum to be three times the lepton momentum for unseen decays.

We have studied the sensitivity of the likelihood functions to the estimates of l_{max} and the D mo-menta for the unseen decays and to the uncer-tainties in the decay distances and D momenta for the observed decays. The effects of the un-certainties in these quantities on the lifetimes are hard to estimate quantitatively but are small compared to the statistical uncertainties for rea-sonable variations in these quantities. Therefore, we have not attempted to include these effects in the quoted limits on the lifetimes. Table VIII gives our lifetime results for three assumed P_{D^0}

TABLE VIII. D^+ and D^0 lifetime determinations.

Particle	Most probable value (10^{-13} sec)	2σ limits Lower (10^{-13} sec)	2σ limits Upper (10^{-13} sec)
D^+ ($P_{D^0} = 0.1$)	$1.8^{+1.7}_{-0.8}$	0.6	7.0
D^0 ($P_{D^0} = 0.1$)	$7.5^{+9.5}_{-4.3}$	1.5	42
D^+ ($P_{D^0} = 0.5$)	$2.2^{+2.3}_{-1.1}$	0.6	10
D^0 ($P_{D^0} = 0.5$)	$2.8^{+2.2}_{-1.3}$	0.9	8.0
D^+ ($P_{D^0} = 0.9$)	$2.7^{+5.1}_{-1.5}$	0.6	27
D^0 ($P_{D^0} = 0.9$)	$1.9^{+1.1}_{-0.8}$	0.7	4.5

values. The lifetimes are approximately linear with P_{D^0} for values between 0.1 and 0.9. The dif-ference between the variation of τ_{D^0} and τ_{D^+} with P_{D^0} is due to the $\frac{2}{3}$ of D^+ decays which yield only one charged particle and are assumed to be un-detectable. For $P_{D^0} = 0.5$ the results are con-sistent with but slightly less than those we deter-mined previously due to the increased event sam-ple.

Our values may be compared to the values ob-tained by the emulsion experiments of $10.3^{+10.5}_{-4.1} \times 10^{-13}$ sec (Ref. 34) or $2.5^{+2.2}_{-1.1} \times 10^{-13}$ sec (Ref. 43) for τ_{D^+} and $1.00^{+0.52}_{-0.31} \times 10^{-13}$ sec (Ref. 34) or $0.53^{+0.57}_{-0.25} \times 10^{-13}$ sec (Ref. 43) for τ_{D^0}. Agreement with the emulsion experiments improves as P_{D^0} increases and is not unreasonable for $P_{D^0} > 0.5$. A value of P_{D^0} greater than 0.5 would require a D^0 production rate larger than that for D^+ because of the difference in the semileptonic branching ratios. Because of the difficulty in uniquely iden-tifying the decaying particles (especially in semi-leptonic modes), another possibility is that the neutral decays we observe are not D^0 decays but are the semileptonic decays of some other short-lived particle—for example, a neutral charmed baryon. Some support for this possibility is given by the Fermilab experiment.[34] Of their ten neutral decays, two have identified protons among the decay products and thus are presumably decays of a neutral, short-lived baryon. Also, it should be noted that their only semileptonic D^0 decay candi-date has a decay time that is a factor of ten larger than the lifetime they would deduce from their six nonleptonic decays.

X. SUMMARY AND CONCLUSIONS

In an experiment using the Fermilab 15-foot bubble chamber exposed to a quadrupole triplet neutrino beam, we found 49 $\mu^- e^+$ events and 14 $\mu^+ e^-$ events giving dilepton-to-single-lepton ratios of $(0.73 \pm 0.11)\%$ and $(1.1 \pm 0.3)\%$, respectively, for

electron momentum greater than 300 MeV/c. The μ^-e^+ rate per charged-current event shows no strong energy dependence in the range from 30 to 300 GeV. Requiring the electron momentum to be greater than 4 GeV/c, we find good agreement with the dimuon results of this experiment.

We observe 13 (1) K_S^0's and 2 (2) Λ in the μ^-e^+ (μ^+e^-) events and obtain corrected rates of 1.2 ± 0.3 ($0.6^{+0.6}_{-0.3}$) strange particles per event.

Our μ^-e^- candidates are consistent with background. We find the μ^-e^-/μ^-e^+ rate to be less than 0.07 at the 90% confidence level.

In addition to the ν_μ dilepton events, we found 5 candidates for ν_e dilepton production: 2 $e^-\mu^+$, 2 e^-e^+, and 1 e^+e^-. The ν_e dilepton rates are approximately 1%, in agreement with the ν_μ rates.

We have compared our μ^-e^+ and μ^+e^- events with a charm production and decay Monte Carlo and obtain good agreement, apart from a possible enhancement at ≈ 6 GeV/c^2 in the mass of the system recoiling against the μ^+ in μ^+e^- (and $\mu^+\mu^-$) events. For our events with $W = 5-6$ GeV/c^2, we see no strong correlation with other kinematic quantities. The lepton-V^0 invariant-mass distribution (using both $\mu\mu$ and μe events) is consistent with either $D \to \bar{K}e\nu$ or 50% $D \to \bar{K}e\nu$ and 50% $D \to \bar{K}^*e\nu$.

We find no strong evidence for K^* production in the $K\pi$ invariant mass distribution but cannot rule out 50% $D \to \bar{K}^*e\nu$.

Combining our μe and $\mu\mu$ strange-particle events, we note that most of the V^0's are K_S^0's, suggesting that the events are predominantly D-meson production and decay and that the $\Lambda_c^+ \to \Lambda e^+X$

branching ratio is very small. The combined neutral-strange-particle rate is 1.0 ± 0.2 per/event. This is consistent with what is expected based on the charm model.

Finally, we have redone our D^+ and D^0 lifetime determinations using our visible decays and complete sample of dilepton events. Our values are in reasonable agreement with those determined by emulsion experiments provided that at least 50% of dilepton events have D^0 decays. Because of the difficulty in uniquely identifying particles that decay semileptonically, it is also possible that the neutral decays we observe are not of D^0 but rather of a neutral charmed baryon.

---

*Now at TRW, Inc., Redondo Beach, California.

†Now at CERN, 1211 Geneva 23, Switzerland.

‡Now at Univ. de Neuchatel, Neuchatel, Switzerland.

§Now at DESY, Hamburg, Germany.

¶Now at Physical Technical Institute, Tashkent, USSR.

[1]J. von Krogh *et al.*, Phys. Rev. Lett. **36**, 710 (1976).

[2]P. Bosetti *et al.*, Phys. Rev. Lett. **38**, 1248 (1977).

[3]J. Blietschau *et al.*, Phys. Lett. **60B**, 207 (1976).

[4]C. Baltay *et al.*, Phys. Rev. Lett. **39**, 62 (1977).

[5]H. C. Ballagh *et al.*, Phys. Rev. Lett. **39**, 1650 (1977).

[6]P. C. Bosetti *et al.*, Phys. Lett. **73B**, 380 (1978).

[7]O. Erriquez *et al.*, Phys. Lett. **77B**, 227 (1978).

[8]J. P. Berge *et al.*, Phys. Lett. **81B**, 89 (1979).

[9]D. S. Baranov *et al.*, Phys. Lett. **81B**, 261 (1979).

[10]H. C. Ballagh *et al.*, Phys. Rev. D **21**, 569 (1980).

[11]N. Armenise *et al.*, Phys. Lett. **86B**, 115 (1979).

[12]N. Armenise *et al.*, Phys. Lett. **94B**, 527 (1980).

[13]A. Benvenuti *et al.*, Phys. Rev. Lett. **34**, 419 (1975).

[14]A. Benvenuti *et al.*, Phys. Rev. Lett **35**, 1199 (1975); **35**, 1203 (1975). **35**, 1249 (1975).

[15]B. C. Barish *et al.*, Phys. Rev. Lett. **36**, 939 (1976); **39**, 981 (1977).

[16]M. Holder *et al.*, Phys. Lett. **69B**, 377 (1977).

[17]A. Benvenuti *et al.*, Phys. Rev. Lett. **41**, 1204 (1978).

[18]M. Murtagh, in *Proceedings of the 1979 International Symposium on Lepton and Photon Interactions at High Energies, Fermilab*, edited by T. B. W. Kirk and H. D. I. Abarbanel (Fermilab, Batavia, Illinois, 1980).

[19]A. Benvenuti *et al.*, Phys. Rev. Lett. **41**, 725 (1978).

[20]M. Holder *et al.*, Phys. Lett. **70B**, 396 (1977).

[21]R. J. Cence *et al.*, Nucl. Instr. Meth. **138**, 245 (1976).

[22]M. L. Stevenson, in *Proceedings of the Topical Conference on Neutrino Physics at Accelerators, Oxford, 1978*, edited by A. G. Michette and P. B. Renton (Rutherford Laboratory, Chilton, Didcot, Oxfordshire, England, 1978), p. 362.

[23]The charged-current efficiencies quoted are somewhat larger than those in Ref. 10 because of the smaller fiducial volume.

[24]The values actually obtained for the μe events were $A = 1.18 \pm 0.11$ and $B = -0.5 \pm 1.5$, which are consistent with the dimuon values.

[25]R. J. Loveless *et al.*, Phys. Lett. **78B**, 505 (1978).

[26]C. -H. Lai, Phys. Rev. D **18**, 1422 (1978).

[27]R. D. Field and R. P. Feynman, Phys. Rev. D **15**, 2590 (1977).

[28]R. Barnett, Phys. Rev. Lett. 36, 1163 (1976); H. Georgi and H. Politzer, *ibid.* 36, 1281 (1976).

[29]V. Barger *et al.*, Phys. Rev. D 16, 746 (1977).

[30]W. Bacino *et al.*, Phys. Rev. Lett. 43, 1073 (1979). They actually find that the fraction of $K\pi e\nu$ is $(37\pm16)\%$ if the $K\pi$ system is entirely $K^*(890)$, or $(55\pm21)\%$ if the $K\pi$ system is nonresonant.

[31]A. Pais and S. Treiman, Phys. Rev. Lett. 35, 1206 (1975).

[32]The difference between the two Monte Carlo predictions for these distributions is caused partially by the use of the bare quark mass ($m_c = 1.5$ GeV/c^2) in Lai's model, rather than the physical mass ($M_D = 1.87$ GeV/c^2).

[33]J. Bell *et al.*, Phys. Rev. D 19, 1 (1979).

[34]N. Ushida *et al.*, Phys. Rev. Lett. 45, 1049 (1980); 45, 1053 (1980).

[35]W. Bacino *et al.*, Phys. Rev. Lett. 45, 329 (1980).

[36]J. Blietschau *et al.*, Phys. Lett. 86B, 108 (1979).

[37]Particle Data Group, Rev. Mod. Phys. 52, S25 (1980).

[38]C. Baltay *et al.*, Phys. Rev. Lett. 42, 1721 (1979).

[39]T. Kitagaki *et al.*, Phys. Rev. Lett. 45, 955 (1980).

[40]J. M. Weiss, Report No. SLAC-PUB-2558, 1980 (unpublished).

[41]H. J. Willutzki, in *Neutrino '79*, proceedings of the International Conference on Neutrinos, Weak Interactions, and Cosmology, Bergen, Norway, 1979, edited by A. Haatuft and C. Jarlskog (Univ. of Bergen, Bergen, 1980).

[42]H. C. Ballagh *et al.*, Phys. Lett. 89B, 423 (1980).

[43]D. Allasia *et al.*, Nucl. Phys. B176, 13 (1980).